Electrochemistry and staging in $La_2CuO_{4+\delta}$

P. Blakeslee, R. J. Birgeneau, F. C. Chou, R. Christianson, M. A. Kastner, Y. S. Lee, and B. O. Wells
Center for Material Science and Engineering and Department of Physics, Massachusetts Institute of Technology, Cambridge, Massachusetts 02139
(Received 9 September 1997)

Measurements are reported of the time dependence of the current during electrochemical oxidation and reduction at a fixed voltage of single crystals and ceramic samples of $La_2CuO_{4+\delta}$. Staging peaks in neutron measurements of the single crystals together with the electrochemical measurements and magnetization measurements confirm that stage $n=6$ corresponds to $\delta=0.055\pm0.05$, the high-δ side of the oxygen-rich–oxygen-poor miscibility gap. Furthermore, stage $n=4$ occurs at a value of δ consistent with $\delta\propto n^{-1}$. For ceramic samples it is shown that two different superconducting compounds are formed depending on the oxidation voltage used. [S0163-1829(98)06421-2]

I. INTRODUCTION

There has been great interest in the high-T_c superconductor $La_2CuO_{4+\delta}$ in part because of proposals that the phase separation into oxygen-rich and oxygen-poor regions for $0.01<\delta<0.055$ is electronically driven. This would add credence to models in which the superconductivity is related to phase separation of charge carriers, which would be frustrated in other materials.[1] However, the recent discovery of superlattice structures perpendicular to the CuO_2 planes,[2–4] analogous to those in graphite intercalation compounds, has raised the possibility that the phase separation is, instead, a result of the staging of the intercalated oxygen; stage n corresponds to a period of n times the underlying c-axis lattice constant. That is, if staged compounds are formed at specific values of δ, with stage number $n(0.01)=\infty$ and a second finite value for $n(0.055)$, then the phase separation is simply interpreted as a natural consequence of the first-order nature of the transition between these compounds.

In early work, samples of $La_2CuO_{4+\delta}$ were typically prepared by annealing either ceramics or single crystals at high temperature and high oxygen pressure.[5] This is adequate to observe the oxygen-poor and oxygen-rich phase separation. More recently, it has been shown that higher values of δ can be achieved using electrochemical oxidation.[6–8] This technique has been used to oxidize the crystals in which staging is seen using neutron scattering.[2] Whereas there is mounting evidence from neutron scattering that only a few commensurate superlattice periodicities or stages are stable, δ has not been measured for the staged crystals. Furthermore, there are no direct thermodynamic measurements determining whether there are specific stable values of δ.

Before our recent work at MIT, studies of the phase diagram of $La_2CuO_{4+\delta}$ have used polycrystalline (ceramic) samples.[9] In such studies δ is determined from thermogravimetric measurements; the sample is weighed while the excess oxygen is driven off by heating in vacuum. However, the neutron measurements require large, $\sim0.1\ cm^3$, single crystals that require months to oxidize. It is not practical to eliminate the oxygen from these in order to carry out thermogravimetric measurements. For this reason we have determined the oxygen content of single crystals using electrochemical techniques.

In this paper we present measurements of the time dependence of the current and the integrated charge during oxidation and reduction of single crystals and ceramic samples of $La_2CuO_{4+\delta}$. Using neutron scattering, we show directly that a crystal with $\delta=0.055\pm0.05$ has a superlattice periodicity corresponding to stage 6, as had been inferred from previous single-crystal diffraction work together with the phase diagram of ceramics. We also show that δ for stage 4 is larger than that for stage 6 by an amount that is at least approximately consistent with the ratio of the stage numbers.

This paper is organized as follows: Section II discusses the sample preparation and measurement techniques used. In Sec. III we present the results of our measurements. These include the time dependence of the electrochemical current, as well as the magnetization and neutron experiments. Section IV contains a discussion of the results and conclusions.

II. EXPERIMENTAL DETAILS

The single crystals are grown using the traveling-solvent floating-zone method.[10] Because this technique uses no crucible, the crystals are purer than those grown by other means. The starting materials for both crystals and ceramics are 99.999% pure powders of La_2O_3 and CuO. Typical crystals have volumes of $\sim0.5\ cm^3$, as grown.

For electrochemical and other measurements small flawless crystals are prepared as follows: Laue x-ray scattering is used to orient a large crystal, and small pieces, 100–200 mg in mass, are then cut with faces parallel to the c axis, normal to the CuO_2 planes. The faces are polished to eliminate pieces that have cracks, since our previous work has shown that cracks generally cause the crystals to crumble during the oxidation process. After polishing, the crystals are etched in a solution of 1% bromine in methanol for about 15 min; this eliminates structural damage caused by polishing.[11] For electrochemical oxidation the crystals are wrapped in platinum gauze which is subsequently attached to a platinum wire.

The ceramic samples are prepared using a standard solid-state reaction method. The stoichiometric mixture of La_2O_3 and CuO powders is ground with an alumina mortar and

pestle and then heated in an alumina or platinum crucible at 850 °C. The powder is then reground and heated at successively higher temperatures, first at 950 °C and then at 1050 °C. The powder is sintered and reground repeatedly until x-ray powder diffraction shows that it is single-phase La_2CuO_4. The powder is then sifted through a 43-μm screen and about 100 mg is pressed into a pellet in a 0.25-in. die at 1.5–2 metric tons in a Carver hydraulic press. Before pressing, a thin platinum wire is inserted into the powder to be used for electrical contact. Two techniques have been used to increase the grain size after this initial pressing. In one, the pellets are compressed in an isostatic oil press at 35 000 psi and then slowly brought back to atmospheric pressure. In the other, the samples are annealed at 900 °C in an oxygen flow for 6 h. Both techniques result in pellets with density ~70% of the crystalline value.

The electrochemical measurements are performed in a cell consisting of three electrodes: the sample, a platinum wire counterelectrode to provide the current, and a Fisher Scientific high-temperature Ag/AgCl reference electrode. The NaOH solution is placed in a Teflon container and stirred to maintain homogeneity of composition and temperature. Although most room temperature reactions, for ceramics, have been done with 1 molar NaOH, it has been found that this creates unacceptably large side reactions at 353 K where the oxidation of crystals is carried out. It is not clear whether this is the consequence of impurities in the NaOH or dissolution of the sample. Therefore, all measurements above room temperature are accomplished with 0.1 molar NaOH using 99.996% pure NaOH and 18 MΩ de-ionized water. By replacing the sample with a platinum wire, we ascertain that this concentration is adequate to provide the ionic current required by the chemical reaction; that is, the resistance of the solution does not limit the reaction. A constant voltage $V_{\rm ref}=V_{\rm samp}-V_{\rm Ag/AgCl}$ is maintained between the sample and the reference electrode while the current through the counterelectrode is measured. $V_{\rm ref}$ is kept below 0.55 V to eliminate decomposition of H_2O.

Ceramic samples can be oxidized in a few days, and the currents are high enough that currents resulting from side reactions are insignificant. However, for single crystals the currents are smaller, and it is sometimes necessary to subtract a background current of ~0.1 μA or less, measured by replacing the sample with a Pt electrode, before calculating the charge.

In the next section we present magnetization results for oxidized crystals and ceramics and neutron results for oxidized single crystals. A Quantum Design superconducting quantum interference device (SQUID) magnetometer is used for measurements of the magnetic moment. Low fields are used to examine the superconducting behavior and high fields to measure the antiferromagnetic component.

The neutron-diffraction experiments have been performed at beam line H9A at the High Flux Beam Reactor at Brookhaven National Laboratory on a triple-axis spectrometer. The incident neutron energy is fixed at 5 meV and a cooled Be filter is used to suppress reflections from higher-order neutrons. The samples are mounted on the spectrometer so that the $(H0L)$ and $(0KL)$ zones are in the scattering plane. Because of twinning, these zones are scanned simultaneously. The notation used here is for the $Bmab$ unit cell, where the c axis is perpendicular to the CuO_2 planes and the a and b axes are 45° from the tetragonal axes. Collimations are typically set at $60'$-$40'$-$15'$-S-$5'$-$10'$ for measuring the strong fundamental peaks and at $60'$-$40'$-$60'$-S-$80'$-$80'$ for measuring the weaker superlattice peaks. The first three collimators are respectively, before, in between, and after the double monochromatizing graphite crystals. A closed-cycle He refrigerator is used to cool the samples.

III. RESULTS

For $V_{\rm ref}$ greater than ~0.25 V, negative current flows into the sample corresponding to oxidation by means of the reaction

$$La_2CuO_4+2\delta OH^-\rightarrow La_2CuO_{4+\delta}+\delta H_2O+2\delta e^-, \quad (1)$$

which is balanced at the counterelectrode by

$$2\delta H_2O+2\delta e^-\rightarrow 2\delta OH^-+\delta H_2. \quad (2)$$

Thus the charge Q passing through the cell is $-2\delta e$. At equilibrium no current flows and $V_{\rm ref}$ is related to the free energy of the reaction through the Nernst equation. Since the free energy is proportional to the chemical potential of oxygen in the sample, δ can in principle be determined as a function of oxygen chemical potential. However, these arguments only apply at equilibrium. One may approach equilibrium by allowing the current to go to zero at fixed $V_{\rm ref}$ or to measure the voltage at sufficiently small currents that the process is quasistatic. We have carried out constant $V_{\rm ref}$ measurements for both single crystals and ceramics. We measure the current as a function of time t and integrate it to determine the charge $Q(t)$ that has passed through the sample. Eventually, Q saturates, at Q_0. Even for these measurements, the equilibrium may be metastable, as appears to be the case in some of our experiments.

For the crystals we begin by removing the ~1% excess oxygen known to be incorporated during growth. When first placed in the NaOH solution, the open circuit voltage of the sample is typically $V_{\rm ref}$~0.18 V. If the voltage is reduced below this value oxygen begins to leave the sample. Such a reduction experiment is illustrated in Fig. 1. We plot the relative deviation of $Q(t)$ from Q_0 to illustrate the exponential time dependence of the approach to equilibrium; Q is measured in electrons per formula unit. The gap in the data results from a temporary interruption in the experiment. In these reduction experiments, the current is initially a few μA.

We have reduced five crystals in this way and typically find that the crystals have δ~0.005 as grown. The values of Q_0 for the reduction experiments, Q_r, and the time constants for the current decay, τ_r, are listed in Table I. One of the samples, XE5, had been annealed in oxygen before electrochemical reduction. For the others Q_r~0.01, which is consistent with previous measurements.[9,12] The time constant is remarkably reproducible from sample to sample with $\tau_r=(1.5\pm0.6)\times10^5$ s$=1.7\pm0.7$ days. The experiment in Fig. 1 is the only one done at 313 K instead of 353 K. Surprisingly, the time constant appears to be independent of temperature over this range.

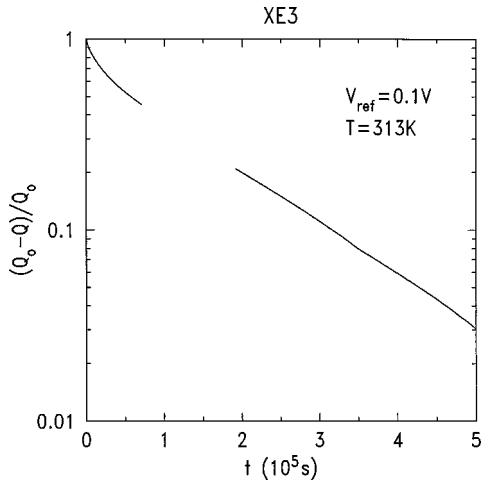

FIG. 1. Deviation of integrated charge from its asymptotic value as a function of time on a semilogarithmic plot during reduction of a single crystal XE3. The time constant is 1.6×10^5 s=1.8 days. The measurement of current was accidentally interrupted between about 1 and 2×10^5 s. This was the only measurement on a single crystal carried out below 350 K.

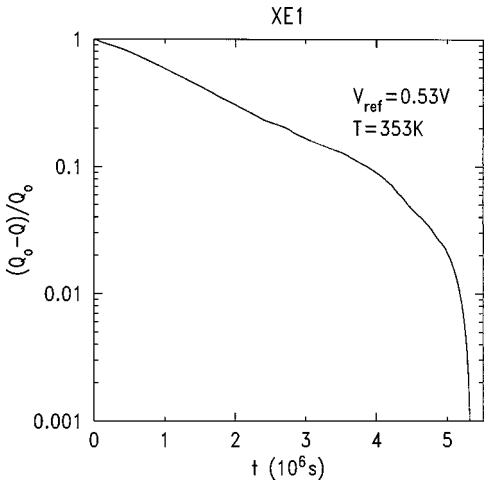

FIG. 2. Semilogarithmic plot of the deviation of the integrated charge from its asymptotic value during oxidation of a single crystal XE1. The time constant is 1.6×10^6=18 days, 10 times longer than the time for reduction (Fig. 1). The downturn at long times is probably the result of a small error in determining Q_0.

After the initial reduction, the crystals were oxidized at various values of $V_{\rm ref}$ as indicated in Table I. A typical measurement of the charge in such an experiment is shown in Fig. 2. For oxidation of single crystals the initial current is typically a few tenths of a μA. The downturn at about 5×10^6 s is the result of a choice of Q_0 that is slightly too large. As for the reduction experiment, the charge approaches its equilibrium value exponentially. However, the time constant for oxidation, τ_0, is about 10 times longer than that for reduction. As seen from Table I, we find time constants ranging from 1 to 3.5×10^6 s or 13–40 days. All oxidation measurements are made at 353 K for the single crystals.

The current $I(t)$ is shown for oxidation of two ceramic samples in Fig. 3. The current is three orders of magnitude higher than that for single crystals. In this case $I(t)$ is plotted on a log-log plot, to illustrate that for both samples the decay of the current is a power law with exponent -1.5 at long times. Note that because the decay is faster than t^{-1}, the charge converges. However, the current for one sample decays much faster than that for the other. The decay may be approximated by the functional form

$$I=I_0(1+t/t_0)^{-1.5}, \tag{3}$$

which means that for Q to reach 90% of Q_0 requires $t\sim100t_0$. For one sample in Fig. 2 $t_0\sim3\times10^3$ s, which means that 90% saturation requires $\sim$3 days. For the second sample, however, saturation would take $\sim$30 days, comparable to the time for the single crystals. For the many ceramic pellets studied we find no correlation between t_0 and $V_{\rm ref}$, and so the variation in t_0 must be the result of sample-to-sample variation. (Some of our measurements on ceramics had been made before we were aware of these long equilibration times and are therefore subject to some uncertainty as noted below.)

Figure 4 illustrates oxidation and reduction experiments for a ceramic pellet at 278 K. The oxidation current is smaller by two or three orders of magnitude than that at room temperature, and the time scale for oxidation is much longer. The time scale for reduction and the magnitude of the current is about the same as for single crystals, and the reduction is much faster than the oxidation. We have not carried out reduction experiments on pellets at higher temperatures.

Because of the very long time scale and its sample-to-sample variation, we have measured $Q_0(V)$ by using one pellet, altering $V_{\rm ref}$ in very small steps and waiting until the current is less than the noise after each step. For most steps this requires about 4 days and results in an uncertainty of about 0.002 electrons per formula unit (e/f.u.). For other experiments, as discussed below, we have used multiple pellets and shorter electrolysis times, but these measurements are consequently subject to greater uncertainties. Figure 5 shows the charge as a function of voltage during oxidation and then reduction. The hysteresis indicates that the equilibria are metastable. The diamonds indicate measurements for which the current does not decay even after about 4 days.

TABLE I. Results of single-crystal electrochemical measurements.

Sample	$V_{\rm ref}$ (V)	Q_r (e/f.u.)	Q_0 (e/f.u.)	τ_r (10^5 s)	τ_0 (10^6 s)
XE2	0.35	0.008±0.002	0.033±0.002	2.1	1.1
XE5	0.40	0.033±0.005	0.075±0.005	0.9	3.3
XE3	0.45	0.008±0.01	0.11 ±0.01	1.6	1.7
XE4	0.45	0.017±0.001	0.063±0.001	0.9	3.5
XE1	0.53	0.007±0.01	0.127±0.01	1.6	1.6

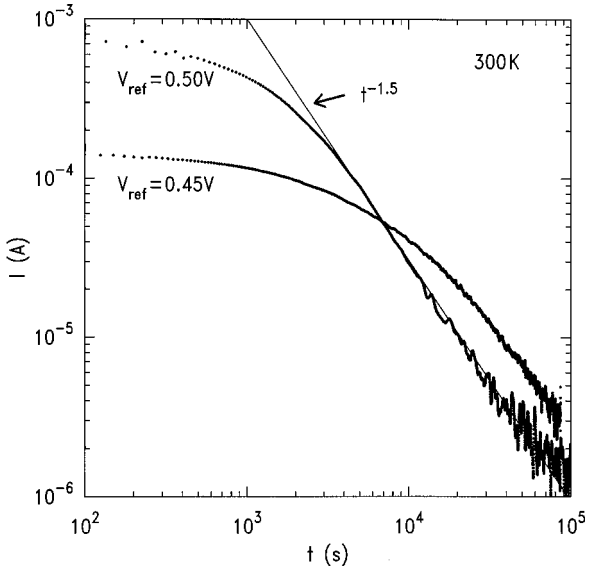

FIG. 3. Log-log plot of current as a function of time during oxidation of two ceramic pellets at room temperature. The differences in the time decay are probably the result of sample-to-sample variation rather than the difference in voltage used. Both samples follow $I \sim t^{-1.5}$ at long times.

From the reduction data in Fig. 5 is clear that there are two plateaus in Q_0 as a function of $V_{\rm ref}$. The one below 0.33 V has $Q_0 = 0.115 \pm 0.002\, e$/f.u. or $\delta = 0.058 \pm 0.001$, and the one above 0.375 V has $Q_0 = 0.127 \pm 0.002\, e$/f.u. or $\delta = 0.064 \pm 0.001$.

Data for oxidation of five single crystals are also plotted in Fig. 5. The large variation in δ for single crystals results from incomplete oxidation, even when the current apparently goes to zero. This becomes clear from magnetization and neutron experiments, as discussed next.

The magnetization divided by the field is plotted for crystal XE1 in Fig. 6. In the upper panel are measurements at 5 Oe to make the superconducting properties manifest. The shielding is large, but the Meissner fraction is very small. The data have not been corrected for demagnetization effects. It is clear from the figure that there are two superconducting components, whose transitions are indicated by arrows. We use the onset of diamagnetism to determine the higher T_c and the change of curvature to estimate the lower T_c. Most of the crystals studied in this work and by Wells *et al.*[2,13] contain only one component with $T_c = 32$ K. However, XE1 also has a component with $T_c \sim 40$ K.

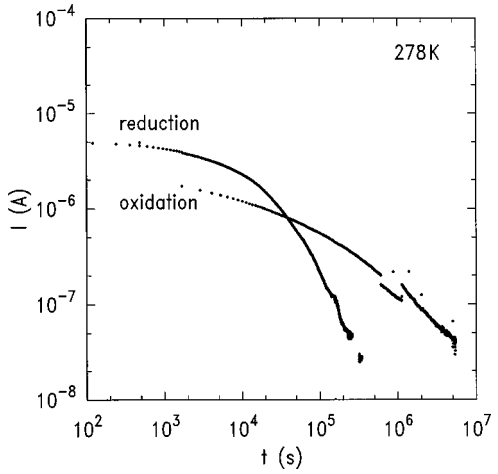

FIG. 4. Log-log plot of current as a function of time during oxidation and reduction of a ceramic pellet at 278 K. The oxidation is slower than at room temperature, but the reduction is faster than the oxidation.

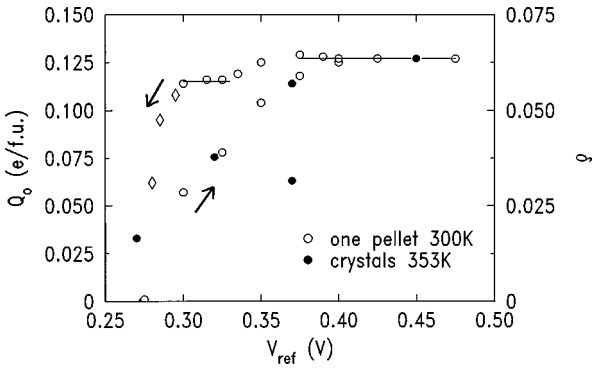

FIG. 5. Asymptotic values of the charge (left) and δ (right) for single crystals and a ceramic pellet. The charge for crystals is that for oxidation, and although it increases with $V_{\rm ref}$, it shows substantial sample-to-sample variation. The data for the ceramic pellet were taken during stepwise oxidation and reduction. Lines are drawn to emphasize the two plateaus seen during reduction. The diamonds correspond to voltages for which the current was too large to obtain even metastable equilibrium.

The small Meissner fraction is the first clue that the sample is inhomogeneous. The lower panel of Fig. 6 makes this very clear: The magnetization measurements at 5×10^4 Oe show the increase in moment below 240 K, characteristic of the Néel transition in lightly doped La_2CuO_4. From previous measurements, one knows that this results from a phase with $\delta \sim 0.005$–0.01.[9] From the size of the weak ferromagnetic moment measured at 5×10^4 Oe, one finds that $\sim$33% of the sample is in this antiferromagnetic

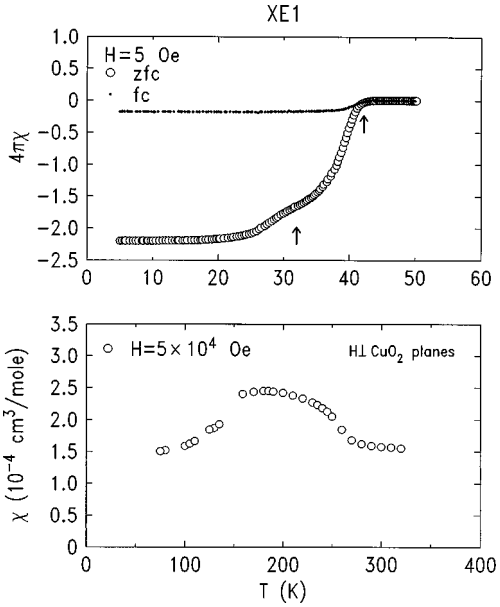

FIG. 6. Upper panel: Meissner and shielding measurements at 5 Oe. Lower panel: magnetic moment at 5×10^4 Oe.

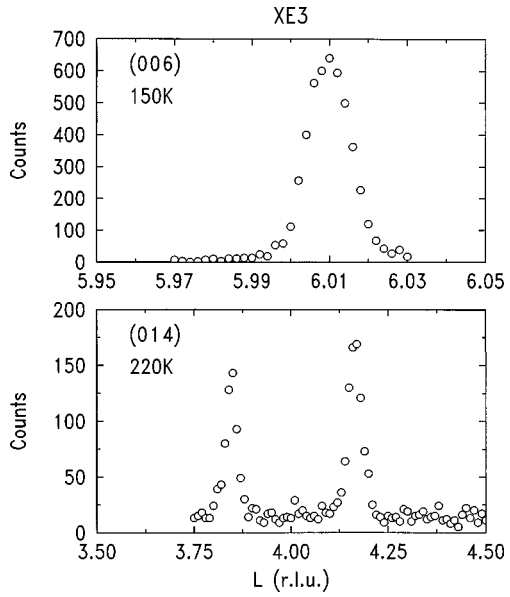

FIG. 7. Neutron-scattering measurements on crystal XE3. Upper panel: scan along L, revealing a single (006) peak, indicating that this crystal is single phase. Lower panel: scan along L near the (014) position, revealing superlattice peaks corresponding to stage $n=6$. The antiferromagnetic phase is absent.

phase. In general, the antiferromagnetic fraction decreases with increasing $V_{\rm ref}$, but there appear to be antiferromagnetic inclusions in some samples that are very difficult to oxidize.

Figure 7 shows neutron-scattering scans along two directions in reciprocal space for crystal XE3. The upper panel, a scan of q along L, shows one (006) Bragg peak corresponding to a single phase. The lower panel shows the two superlattice peaks resulting from a splitting of the (014) Bragg peak. The latter peak results from the ordered tilting of the

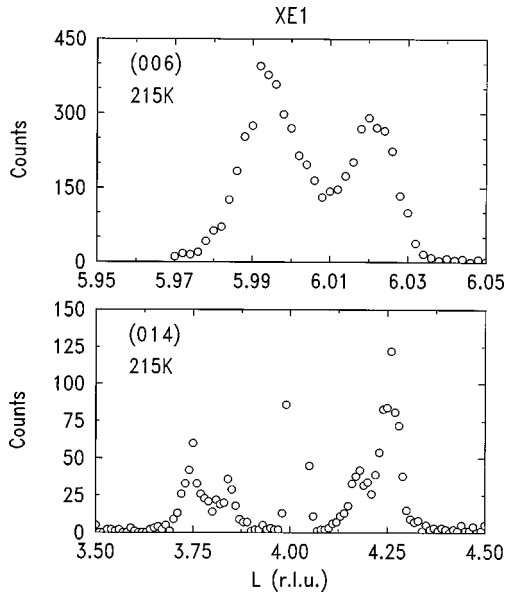

FIG. 8. Neutron-scattering measurements on crystal XE1. Upper panel: scan along L reveals two (006) peaks. Lower panel: scan along L near (014) reveals the central peak from the antiferromagnetic phase, small stage $n=6$ peaks and larger $n=4$ peaks.

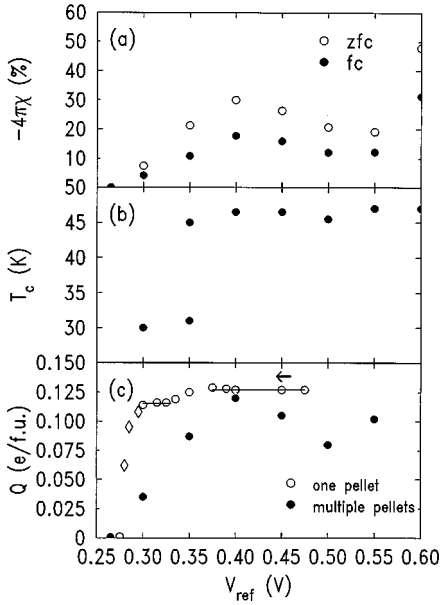

FIG. 9. Correlation between superconducting transition temperature and oxygen content of multiple pellets. Each pellet was oxidized for 1 day, and the integrated charge is plotted as solid circles in (c). The data for the single pellet are also plotted for comparison. As in Fig. 5, the diamonds correspond to voltages for which the current was too large to obtain equilibrium. This 1-day oxidation is not adequate to reach equilibrium, which is probably the reason for the sample-to-sample variation seen. The Meissner and shielding fractions measured are shown in (a), and the T_c determined from the onset of diamagnetism is shown in (b). Note that T_c increases from 32 to 45 K at the same voltage at which the step is seen in the one-pellet data.

CuO_6 octahedra in the orthorhombic phase, and the peak splits in $La_2CuO_{4+\delta}$ when staging occurs.[2–4] The positions of the (014) peaks in Fig. 7 correspond to stage $n=6$.

In Fig. 8 are equivalent scans for crystal XE1, the one for which magnetization measurements are shown in Fig. 6. The upper panel shows two c-axis lattice constants; the smaller (larger q) comes from the antiferromagnetic oxygen-poor phase, and the larger (smaller q) comes from the oxygen-rich phase. From the heights and widths of the peaks, we estimate that less than 40% of the sample is in the oxygen-poor phase. This is consistent with the magnetization measurements which imply that $\sim$33% of the sample is in the antiferromagnetic phase. The oxygen-rich phase contains a stage-4 phase as well as a stage-6 phase. The (014) Bragg peak from the oxygen-poor phase and the superlattice peaks are seen in the lower panel.

Although only $T_c=32$ K is seen for most single crystals studied here and by Wells *et al.*[2,13], which are oxidized below 0.55 V, higher values of T_c are found for ceramic pellets. The middle panel of Fig. 9 shows T_c for a set of pellets, each oxidized for 1 day. The T_c increases at 0.35 V, and the sample oxidized at 0.35 V shows two transitions. The higher T_c is 45 K for ceramics oxidized at room temperature and 41 K for those oxidized at 353 K. These are determined in the same manner as discussed above for crystal XE1.

The lower panel compares the charge for multiple pellets with that for the one pellet measured as oxygen is removed. The sample-to-sample variation for multiple pellets results in

part from the relatively short time of oxidation. It seems clear that the increase in T_c corresponds to the increase in charge, i.e., δ, at 0.35 V. The top panel of Fig. 9 shows the Meissner and shielding fractions.

IV. DISCUSSION AND CONCLUSIONS

It has been suggested that the oxidation of La_2CuO_4 is diffusion limited. This situation would be closely analogous to the oxidation of copper studied by Bardeen, Brattain, and Shockley.[14] In the latter case the reaction is limited by diffusion of vacancies through the growing surface oxide, whereas in $La_2CuO_{4+\delta}$ it would be limited by interstitials diffusing through the oxygen-rich surface layer. However, the observed time dependence and time scale for saturation of the charge are difficult to reconcile with this model. Arrouy *et al.*[15] have found that the time dependence of the electrochemical current during oxidation of ceramics at short times exhibits $t^{-1/2}$ behavior, as expected for a diffusion-limited process.[14,16] We find a similar time dependence for ceramics at times less than $\sim 10-45$ min after oxidation begins. From the latter measurements we would estimate diffusion coefficients of $D \sim 10^{-10}-10^{-11}$ cm^2/s; those of Arrouy *et al.* give $10^{-13}-10^{-14}$ cm^2/s. However, with such small values of D the mm-size single-crystal samples would equilibrate only after 10^8-10^{12} s, whereas we observe time constants of order 10^6 s. Furthermore, the crystals show neither the $t^{-1/2}$ dependence nor the activated temperature dependence characteristic of diffusion-limited surface oxidation.[16] Nonetheless, as one approaches equilibrium, one expects the observed exponential time decay of the current. Using the exponential time constant τ_r for reduction of the crystals, one finds a very large diffusion coefficient in the lightly doped regime $\sim 10^{-6}$ cm^2/s. Thus it is difficult to reconcile the rapid oxidation and reduction with a diffusion-limited process.

One might have argued that electric fields accelerate the movement of oxygen ions in La_2CuO_4. However, even at 278 K the dielectric relaxation time resulting from motion of holes created by oxygen doping is very small[12,17] and any electric field would be screened. This is taken into account in the theory of Bardeen *et al.*[14] Alternatively, one might have argued that inhomogeneous strain accelerates diffusion. However, we find even shorter equilibration times for the reduction of lightly doped samples, which have almost the same lattice constant as the undoped material, than for the oxidation of samples, for which the difference in strain at the boundary between oxygen-rich and oxygen poor regions is large. We have no model to explain the rapid equilibration of the oxidation and reduction reactions.

Our combined neutron, magnetization, and electrochemical data provide additional information about the phase diagram of $La_2CuO_{4+\delta}$. The miscibility gap between the antiferromagnet and the oxygen-rich phase [the antiferromagnetic (AF) gap] is between $\delta=0.01$ and $\delta=0.055$ for ceramic samples. Wells *et al.* have studied a crystal with δ in the AF gap which shows phase separation and staging with stage $n=6$ as T is lowered. From this they infer that $n=6$ at $\delta=0.055$, the high-δ edge of the AF gap. They could not determine this directly because δ is not known for their crystal. Crystal XE3 has only stage-6 superlattice peaks, no antiferromagnetic phase (Fig. 7), and a charge of $Q_0=0.11\pm0.01\,e$/f.u., corresponding to $\delta=0.055\pm0.05$, thus confirming that stage 6 occurs at this value of δ.

Crystal XE1 (Fig. 6) has a component that is antiferromagnetic with $T_N=240$ K, corresponding to $\delta=0.005-0.01$. Using the size of the weak ferromagnetic moment to determine the antiferromagnetic fraction (Fig. 6), we conclude that the oxygenated portion of XE1, which contains both stage 6 and stage 4, has $\delta=0.1\pm0.01$. Assuming that stage 6 occurs only for $\delta=0.055$ and using the intensities of the neutron peaks (Fig. 8, lower panel), we estimate that stage 4 is at $\delta=0.11\pm0.02$. A proper two-dimensional integration of the neutron peaks might alter this number somewhat. Thus we conclude that $n=6$ is at $\delta=0.055\pm0.005$ and $n=4$ is at $\delta=0.11\pm0.02$, so that the ratio of δ's is 2 ± 0.6. This ratio of the δ's is consistent with the simple ratio 3/2 of the inverse stage numbers, assuming that the in-layer density is independent of stage.

The simple staging model used for graphite intercalation compounds assumes that intercalants have constant density within each layer they occupy, since only $1/n$ layer is occupied by intercalants $\delta \propto n^{-1}$. This has also been found to hold for staging in La_2NiO_4 by Tranquada *et al.*[18] However, there is as yet no way to measure the in-layer density in La_2CuO_4 because scattering from the oxygen itself has not been unambiguously observed. Although we see plateaus in the charge for ceramics, the data for the crystals are inadequate to conclude that each staged phase occurs at a single value of the charge.

It appears that in electrochemically oxidized ceramics of $La_2CuO_{4+\delta}$ two superconducting compounds are formed, one with $T_c=32$ K for $V_{\rm ref}<0.35$ V and the other with $T_c=45$ K for $V_{\rm ref}>0.35$ V. The step-by-step reduction experiment reveals two plateaus in the density of excess oxygen as a function of the voltage, and the step between the plateaus coincides with the change in T_c.

Unfortunately, the results on ceramics and single crystals seem contradictory. We would have expected to see plateaus for the ceramics with charges corresponding to 0.11 ($\delta=0.055$) and 0.165 e/f.u. ($\delta=0.0825$), corresponding to stage 6 and stage 4, respectively. The lower plateau in Fig. 5 is consistent with stage 6, but the upper plateau has a somewhat lower charge than that expected for a saturated stage 4. It may be that the charge is not fully saturated even after the long times used for oxidation. However, even if the ceramic were single-phase stage 4, we would not expect the observed high T_c (~ 45 K) based on the results for crystals. Wells *et al.*[2] have reported $T_c=32$ K for crystals whether stage 6 or stage 4 when oxidized at voltages less than ~ 0.5 V. A phase with T_c above 40 K has only been previously reported in single crystals that have stage 2 and stage 3, which are oxidized at voltages up to 0.6 V.[2] However, the results for crystal XE1 reported here and more recent work by our group suggest that crystals with stage 4 sometimes have a component with $T_c \sim 40$ K. More work needs to be done to identify the structure of phases with T_c greater than ~ 30 K.

It is evident from Fig. 5 that plateaus are more easily identified in reduction than oxidation data. This clearly suggests that it would be valuable to oxidize ceramics and crystals at high voltages, ~ 0.6 V, and then measure δ during

reduction. Although this would give more information about the phase diagram, as for thermogravimetric analysis it would leave a reduced sample.

Doping La_2CuO_4 with excess oxygen has recently been found to give the same incommensurate spin correlations as doping with Sr.[13] Since the oxygen atoms are mobile at much lower temperatures than the Sr impurities, one expects that the oxygen-doped samples are less disordered and, therefore, may provide an advantage in understanding the connection between the antiferromagnetic spin fluctuations and superconductivity. Our work shows that electrochemical measurements of the oxygen content can be valuable in characterizing samples for such studies.

ACKNOWLEDGMENTS

The work at MIT was supported by the MRSEC Program of the National Science Foundation under Grant No. DMR 94-00334 and by NSF Grant Nos. DMR 94-1174 and DMR 97-04532. Part of this study was performed at Brookhaven National Laboratory, which is supported by the Department of Energy under Contract No. DE-AC02-98CH10886.

[1] V. J. Emery, S. A. Kivelson, and H. Q. Lin, Phys. Rev. Lett. **64**, 475 (1990).

[2] B. O. Wells, R. J. Birgeneau, F. C. Chou, Y. Endoh, D. C. Johnston, M. A. Kastner, Y. S. Lee, G. Shirane, J. M. Tranquada, and K. Yamada, Z. Phys. B **100**, 535 (1996).

[3] X. Xiong, P. Wochner, S. C. Moss, Y. Cao, K. Koga, and M. Fujita, Phys. Rev. Lett. **76**, 2997 (1996).

[4] X. Xiong, Q. Zhu, Z. G. Li, S. C. Moss, H. H. Feng, P. H. Hor, D. E. Cox, S. Bhavaraju, and A. J. Jacobson, J. Mater. Res. **11**, 2121 (1996).

[5] J. D. Jorgensen, B. Dabrowski, Shiyan Pei, D. G. Hinks, L. Soderholm, B. Morosen, J. E. Schriber, F. L. Venturini, and D. S. Ginley, Phys. Rev. B **38**, 11 337 (1988).

[6] A. Wattiaux, J. Park, J. Grenier, and M. Pouchard, C. R. Acad. Sci., Ser. II: Mec. Phys., Chim., Sci. Terre Univers **310**, 1047 (1990).

[7] J.-C. Grenier, N. Lagueyte, A. Wattiaux, J.-P. Doumerc, and P. Dordor, Physica C **202**, 209 (1992).

[8] J.-C. Grenier, A. Wattiaux, and M. Pouchard, in *First International Workshop on Phase Separation in Cuprate Superconductors*, edited by E. Sigmund and K. A. Muller (World Scientific, Erice, Italy, 1992), p. 187.

[9] P. G. Radaelli, J. D. Jorgensen, and R. Kleb, Phys. Rev. B **49**, 6239 (1994).

[10] I. Tanaka and H. Kojima, Nature (London) **337**, 21 (1989).

[11] J. P. Falck, A. Levy, M. A. Kastner, and R. J. Birgeneau, Phys. Rev. Lett. **69**, 1109 (1992).

[12] C. Y. Chen, R. J. Birgeneau, M. A. Kastner, N. W. Preyer, and T. Thio, Phys. Rev. B **43**, 392 (1991).

[13] B. O. Wells, Y. S. Lee, M. A. Kastner, R. J. Christianson, R. J. Birgeneau, K. Yamada, Y. Endoh, and G. Shirane, Science **277**, 1067 (1997).

[14] J. Bardeen, W. H. Brattain, and W. J. Shockley, J. Chem. Phys. **14**, 714 (1946).

[15] F. Arrouy, J.-P. Locquet, E. Williams, E. Machler, R. Berger, C. Gerber, C. Monroux, J.-C. Grenier, and A. Wattiaux, Phys. Rev. B **54**, 7512 (1996).

[16] W. Jost, *Diffusion in Solids, Liquids and Gases* (Academic, New York, 1952).

[17] C. Y. Chen, N. W. Preyer, P. J. Picone, M. A. Kastner, H. P. Jenssen, D. R. Gabbe, A. Cassanho, and R. J. Birgeneau, Phys. Rev. Lett. **63**, 2307 (1989).

[18] J. M. Tranquada, Y. Kong, J. E. Lorenzo, D. J. Buttrey, D. E. Rice, and V. Sachan, Phys. Rev. B **50**, 6340 (1994).